Numerical modeling of a hyperthermia therapy using dual-phase-lag model of bioheat transfer

Ewa Majchrzak and Łukasz Turchan*

Department of Strength of Materials and Computational Mechanics, Silesian University of Technology
Konarskiego 18a, 44-100 Gliwice, Poland
e-mail: ewa.majchrzak@polsl.pl, lukasz.turchan@polsl.pl

Abstract

The 3D domain including healthy tissue and tumor region is considered. Heat transfer processes proceeding in this domain are described by the dual-phase lag equation (DPLE). The external heating of tissue is taken into account by the introduction of source function appearing in the energy equation. The DPLE supplemented by boundary and initial conditions is solved by means of the finite difference method. The temperature field obtained allows one to determine the thermal dose TD. On the basis of the value of TD it is possible to estimate the sub-domain of total necrosis inside the tumor. In the final part of the paper the examples of computations are shown.

Keywords: heat transfer, biomechanics, numerical analysis, finite difference methods

1. Introduction

Hyperthermia is a type of cancer treatment in which the body tissue is exposed to high temperature (42-46°C) in order to damage and kill cancer cells. During this treatment the heat is addressed to a small area, such as a tumor, using various techniques e.g. radiofrequency, microwave or ultrasound [1, 5]. The ability to predict the temperature of tumor and surrounding tissue is very important and it is possible, among others, using the methods of numerical modelling. In particular, the thermal dose can be calculated on the basis of temperature distribution and next the domain of total necrosis can be estimated.

2. Formulation of the problem

The domain including healthy tissue Ω_1 and tumor region Ω_2 is a cube with edge length of 0.05 m, while the heating zone within the tumor is a centrally located cube with edge length of 0.01 m, as shown in Fig 1. Temperature field in the domain considered is described by the DPLE [3, 4, 6] and under the assumption that the thermophysical parameters of tumor and healthy tissue are the same it is the following equation

$$c\left[\frac{\partial T}{\partial t}+\tau_q\frac{\partial^2 T}{\partial t^2}\right]=\lambda\nabla^2 T+\lambda\tau_T\frac{\partial\nabla^2 T}{\partial t}+G_B c_B\left(T_B-T\right)+Q_{met}+$$
$$+Q_{ex}-\tau_q G_B c_B\frac{\partial T}{\partial t}+\tau_q\frac{\partial Q_{ex}}{\partial t} \tag{1}$$

where λ is the thermal conductivity, c is the volumetric specific heat, G_B is the perfusion coefficient, c_B is the volumetric specific heat of blood, T_B is the blood temperature, τ_q, τ_T are the relaxation time and thermalization time, respectively, Q_{met} is the metabolic heat source, $T = T(x, y, z, t)$ denotes the temperature, and $Q_{ex} = Q_{ex}(x, y, z, t)$ is the capacity of internal heat sources associated with the external heating of tissue.
It is assumed that [5]

$$\left(x,y,z\right)\in\Omega_2:\quad Q_{ex}=\begin{cases}Q_0, & t\le t_{ex}\\ 0, & t>t_{ex}\end{cases} \tag{2}$$

while for $(x, y, z)\in\Omega_1$: $Q_{ex} = 0$. In formula (2) Q_0 is the constant value and t_{ex} is duration of heating.
The equation (1) is supplemented by boundary condition in the form of adiabatic one (the external heating is taken into account by introduction of internal source function). So

$$\left(x,y,z\right)\in\Gamma:\quad n\cdot\nabla T=0 \tag{3}$$

where n is the normal outward vector. The initial conditions are the following

$$t=0:\quad T=T_p,\quad \frac{\partial T}{\partial t}=0 \tag{4}$$

where T_p is the initial temperature of tissue.

It should be pointed out that for $\tau_T = 0$ the DPL (1) reduces to the Cattaneo-Vernotte equation, while for $\tau_q = \tau_T = 0$ the DPL equation reduces to the Pennes one [3].

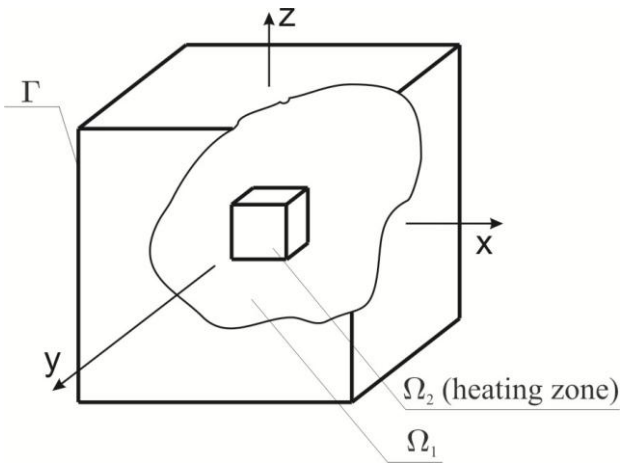

Figure 1: Domain considered

Knowledge of the time-dependent temperature field during thermal treatment allows one to determine the thermal dose TD in terms of equivalent minutes at temperature 43°C.

+ This paper is a part of Grant No N N501 3667 34.

In particular, the following equation should be taken into account [1,4]

$$\mathrm{TD} = \int_{t^0}^{t^F} R^{43-T}\mathrm{d}t = \sum_{f=1}^{F} R^{43-T^f}\,\Delta t \tag{5}$$

where t^0, t^F correspond to the initial and final times, respectively, T^f is the temperature at the point considered for time t^f, $R = 0$ for $T \le 39$°C, $R = 0.25$ for 39°C $< T <$ 43°C and $R = 0.5$ for $T \ge 43$°C.
The TD value required for total necrosis in a case of muscle tissue (this type of soft tissue is considered here) is equal to TD = 240 minutes [1].

3. Method of solution

The problem formulated has been solved using the finite difference method for hyperbolic equations. Taking into account the form of source function , the equation (1) can be written as follows

$$\left(c+\tau_q G_B c_B\right)\frac{\partial T}{\partial t} + c\tau_q\frac{\partial^2 T}{\partial t^2} = \lambda\nabla^2 T + \lambda\tau_T\frac{\partial \nabla^2 T}{\partial t} - G_B c_B T + G_B c_B T_B + Q_{met} + Q_e \tag{6}$$

where Q_e is the non-zero component only for $(x, y, z) \in \Omega_2$ and $t \le t_{ex}$ and then $Q_e = Q_0$. Let $T^f = T(x, y, z, f\,\Delta t)$, where Δt is the time step. Then, for time $t^f = f\,\Delta t$ ($f \ge 2$) the following approximate form of equation (6) can be proposed

$$\left(c+\tau_q G_B c_B\right)\frac{T^f - T^{f-1}}{\Delta t} + c\tau_q\frac{T^f - 2T^{f-1} + T^{f-2}}{(\Delta t)^2} = \lambda\nabla^2 T^{f-1} + \lambda\tau_T\frac{\nabla^2 T^{f-1} - \nabla^2 T^{f-2}}{\Delta t} - G_B c_B T^{f-1} + G_B c_B T_B + Q_{met} + Q_e \tag{7}$$

From initial conditions (4) results that $T^0 = T(x, y, z, 0) = T_p$ and $T^1 = T(x, y, z, \Delta t) = T_p$, of course.
The uniform grid of dimensions $n \times n \times n$ is introduced and then the finite difference equation for internal node (x_i, y_j, z_k) has the following form

$$\left(c+\tau_q G_B c_B\right)\frac{T^f_{i,j,k} - T^{f-1}_{i,j,k}}{\Delta t} + c\tau_q\frac{T^f_{i,j,k} - 2T^{f-1}_{i,j,k} + T^{f-2}_{i,j,k}}{(\Delta t)^2} = \lambda\left(1+\frac{\tau_T}{\Delta t}\right)\nabla^2 T^{f-1}_{i,j,k} - \frac{\lambda\tau_T}{\Delta t}\nabla^2 T^{f-2}_{i,j,k} - G_B c_B T^{f-1}_{i,j,k} + G_B c_B T_B + Q_{met} + Q_e \tag{8}$$

where

$$\nabla^2 T^s_{i,j,k} = \frac{T^s_{i-1,j,k} - 2T^s_{i,j,k} + T^s_{i+1,j,k}}{h^2} + \frac{T^s_{i,j-1,k} - 2T^s_{i,j,k} + T^s_{i,j+1,k}}{h^2} + \frac{T^s_{i,j,k-1} - 2T^s_{i,j,k} + T^s_{i,j,k+1}}{h^2} \tag{9}$$

while $s = f - 1$ or $s = f - 2$ and h is the grid step.
From equation (8) results that

$$\left[\frac{c+\tau_q G_B c_B}{\Delta t} + \frac{c\tau_q}{(\Delta t)^2}\right]T^f_{i,j,k} = \left[\frac{c+\tau_q G_B c_B}{\Delta t} + \frac{2c\tau_q}{(\Delta t)^2} - \frac{6\lambda}{h^2}\left(1+\frac{\tau_T}{\Delta t}\right) - G_B c_B\right]T^{f-1}_{i,j,k} + \frac{\lambda}{h^2}\left(1+\frac{\tau_T}{\Delta t}\right)\cdot \left(T^{f-1}_{i-1,j,k} + T^{f-1}_{i+1,j,k} + T^{f-1}_{i,j-1,k} + T^{f-1}_{i,j+1,k} + T^{f-1}_{i,j,k-1} + T^{f-1}_{i,j,k+1}\right) - \frac{\tau_T\lambda}{h^2\Delta t}\left(T^{f-2}_{i-1,j,k} + T^{f-2}_{i+1,j,k} + T^{f-2}_{i,j-1,k} + T^{f-2}_{i,j+1,k} + T^{f-2}_{i,j,k-1} + T^{f-2}_{i,j,k+1}\right) + \left(\frac{6\tau_T\lambda}{h^2\Delta t} - \frac{c\tau_q}{(\Delta t)^2}\right)T^{f-2}_{i,j,k} + G_B c_B T_B + Q_{met} + Q_e \tag{10}$$

It should be pointed out that in the case of explicit scheme application a criterion of stability should be formulated. The solving system is stable if the coefficients in the difference equations for time t^{f-1} are non-negative. Hence it results that the following coefficient must be positive

$$\frac{-\left(6\lambda + G_B c_B h^2\right)(\Delta t)^2}{h^2\left[\Delta t\left(c+\tau_q G_B c_B\right) + c\tau_q\right]} + \frac{\left(ch^2 + \tau_q G_B c_B h^2 - 6\lambda\tau_T\right)\Delta t + 2h^2 c\tau_q}{h^2\left[\Delta t\left(c+\tau_q G_B c_B\right) + c\tau_q\right]} \ge 0 \tag{11}$$

(the remaining ones are always positive). The nonequality (11) allows to determine the proper time step Δt.

4. Results of computations

At the stage of numerical computations the following values of parameters have been assumed: thermal conductivity of tissue $\lambda = 0.5$ [W/(mK)], volumetric specific heat of tissue $c = 4\cdot10^6$ [W/(m^{3}K)], volumetric specific heat of blood $c_B = 3.9662\cdot10^6$ [J/(m^{3}K)], perfusion coefficient $G_B = 0.0005$ [1/s], metabolic heat source $Q_{met} = 250$ [W/m^3], blood temperature $T_B = 37$°C, relaxation time $\tau_q = 15$ [s], thermalization time $\tau_T = 10$ [s]. The initial temperature is equal to $T_p = 37$°C.
The problem has been solved by means of the finite difference method. The number of nodes was equal to 50×50×50, time step $\Delta t = 0.05$ s.

The following heating conditions are considered [5]: 2 s heating with a power density of 50 [MW/m^3] (variant 1), 10 s heating with a power density of 10 [MW/m^3] (variant 2) and 50 s heating with a power density of 2 [MW/m^3] (variant 3). All of these heating conditions have the same input energy 100 [MJ/m^3].

In the table 1 the maximum temperatures obtained for each variant of computations are collected.

Table 1: Maximum temperatures - DPL model

	Max. temperature [°C]	Time [s]
Variant 1	57.2971	34.35
Variant 2	57.2170	38.55
Variant 3	55.4537	64.25

It should be pointed out that the Pennes equation which is widely used in numerical modelling of bioheat transfer is the special case of DPL equation – for $\tau_q = \tau_T = 0$ the DPL and Pennes equations are the same. To compare the results obtained in two ways, in Fig. 2 the temperature history at the central node of cube for DPL model and successive variants of heating is presented, while Fig. 3 shows the temperature history at the same node for Pennes model and the same variants of heating. In the table 2 the maximum temperatures obtained for each variant of computations using the Pennes model are collected.

In Figures 4 and 5 the temperature distribution at the central cross section for both models is presented.

Figures 6-8 illustrate the temperature distribution in octant of domain obtained using the DPL model, while Figures 9-11 show the temperature distribution in this part of domain obtained using the Pennes model.

In Figures 12, 13 the courses of thermal dose for both models and three variants of heating are presented. In Figures 14, 15 the distribution of thermal dose in the domain considered is shown, while in the Table 3 the degrees of tumor necrosis for each variant analysed are collected.

Table 2: Maximum temperatures - Pennes model

	Max. temperature [°C]	Time [s]
Variant 1	61.988	2
Variant 2	61.876	10
Variant 3	57.755	50

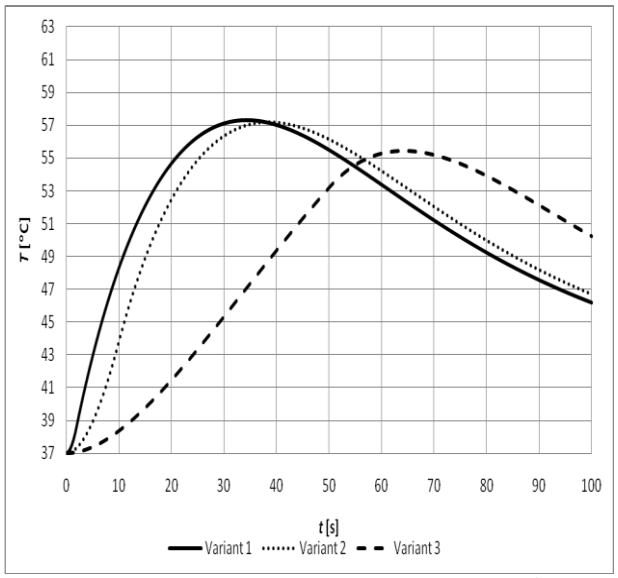

Figure 2: Temperature history at the central point for three variants of heating (DPL model)

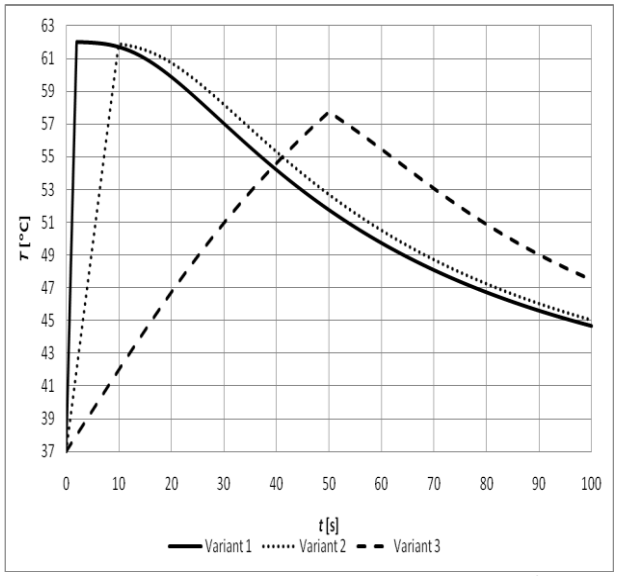

Figure 3: Temperature history at the central point for three variants of heating (Pennes model)

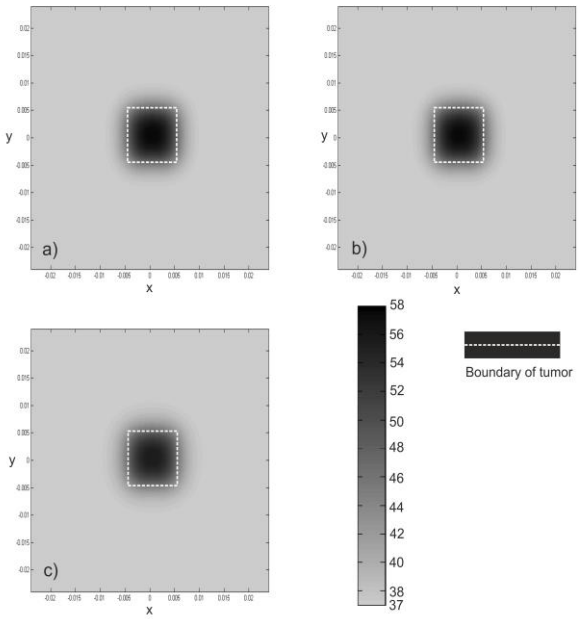

Figure 4: Temperature distribution at the cross section (*xy*, *z* = 0) - DPL model a) variant 1 (*t* = 34.35s), b) variant 2 (*t* = 38.55s), c) variant 3 (*t* = 64.25s)

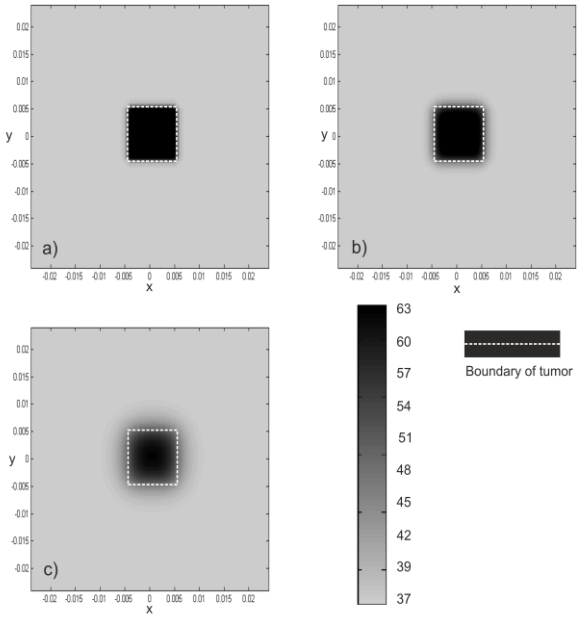

Figure 5: Temperature distribution at the cross section (*xy*, *z* = 0) - Pennes model a) variant 1 (*t* = 2s), b) variant 2 (*t* = 10s), c) variant 3 (*t* = 50s)

Table 3: Degree of the tumor necrosis

Model	DPL	Pennes
Variant 1	31 %	89 %
Variant 2	31 %	65 %
Variant 3	18 %	28 %

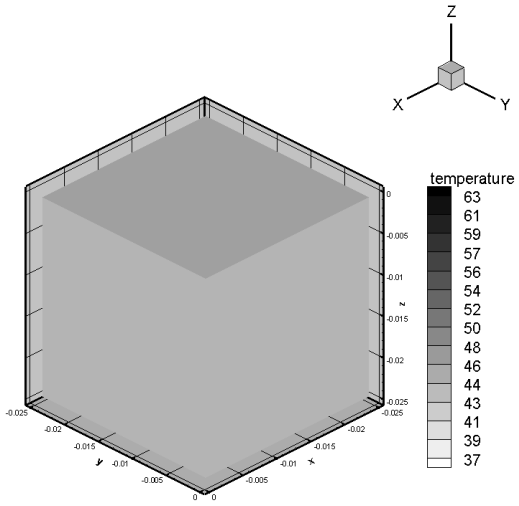

Figure 6: Temperature distribution (t = 10 s, variant 3, DPL model)

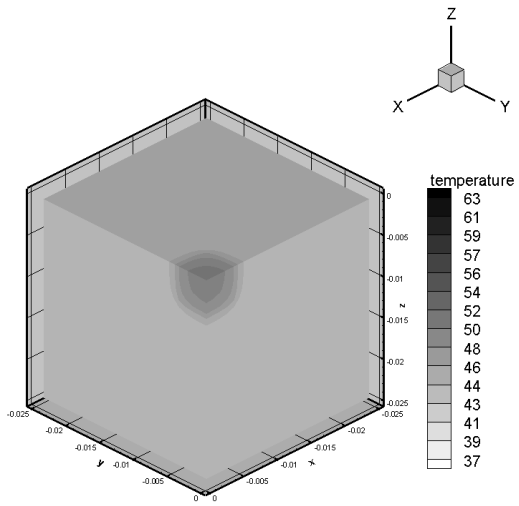

Figure 7: Temperature distribution (t = 30 s, variant 3, DPL model)

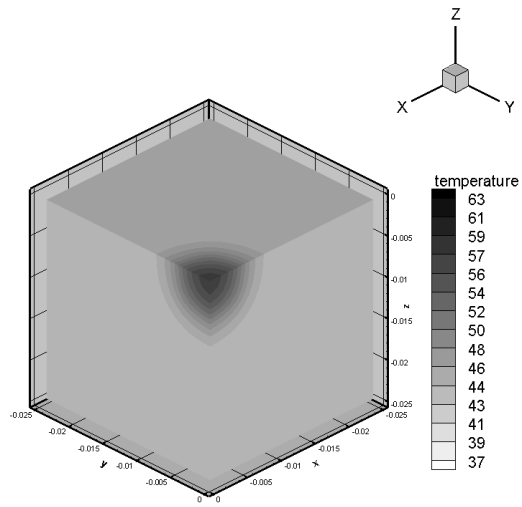

Figure 8: Temperature distribution (t = 70 s, variant 3, DPL model)

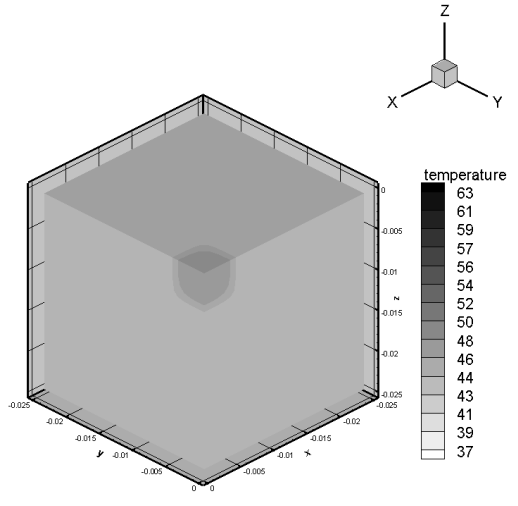

Figure 9: Temperature distribution (t = 10 s, variant 3, Pennes model)

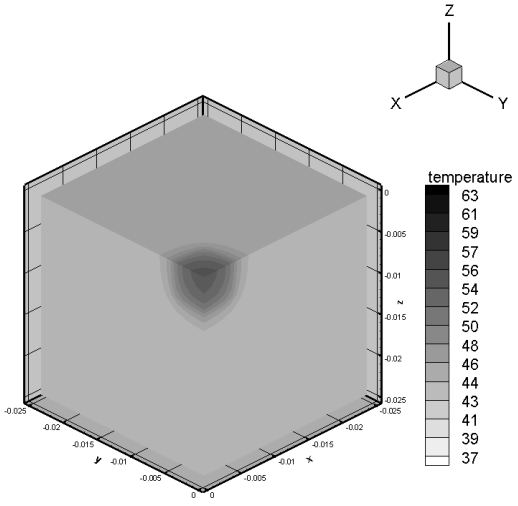

Figure 10: Temperature distribution (t = 30 s, variant 3, Pennes model)

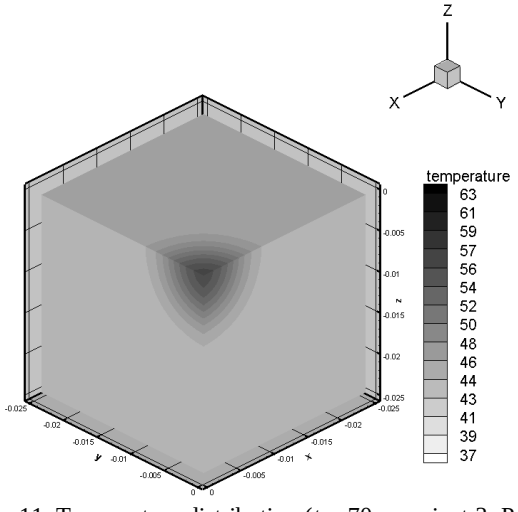

Figure 11: Temperature distribution (t = 70 s, variant 3, Pennes model)

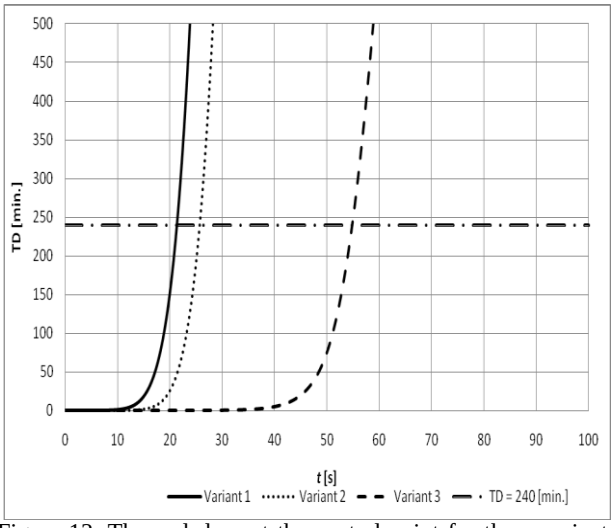

Figure 12: Thermal dose at the central point for three variants of heating (DPL model)

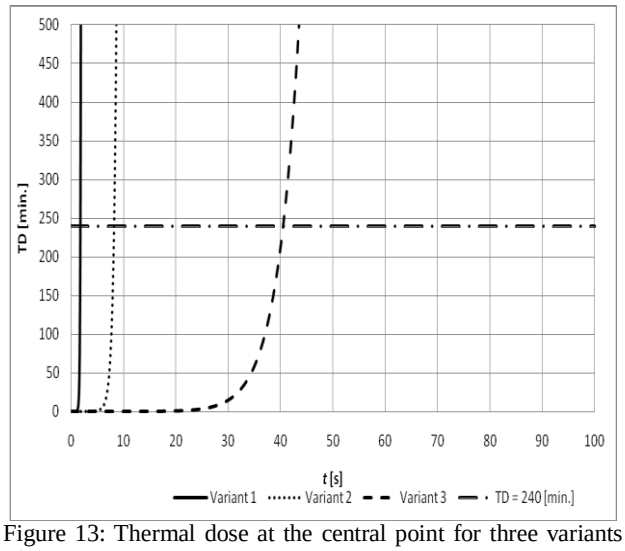

Figure 13: Thermal dose at the central point for three variants of heating (Pennes model)

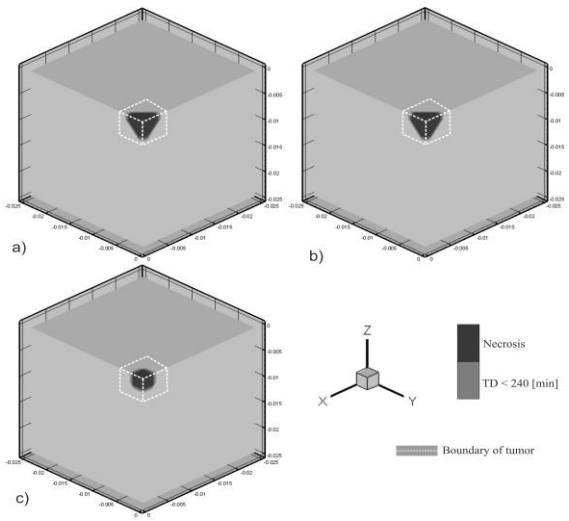

Figure 14: Thermal dose distribution after 100s - DPL model: a) variant 1, b) variant 2, c) variant 3

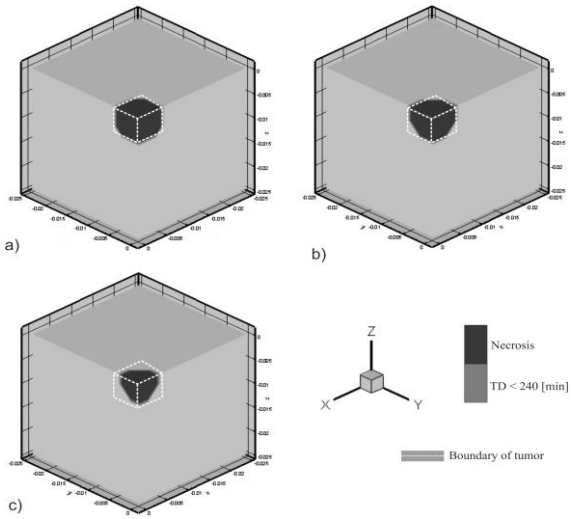

Figure 15: Thermal dose distribution after 100s - Pennes model: a) variant 1, b) variant 2, c) variant 3

5. Conclusions

For a patient, the long duration of heating at high temperature will induce a feeling of discomfort and pain [5]. This is one of the reasons why rapid hyperthermia therapy is preferable. On the other hand, for the short duration of heating the differences between predicted temperatures resulting from the application of DPL equation and Pennes one are greatest. So, in the place of widely used Pennes equation the dual-phase-lag equation should be applied because it takes into account the nonhomogeneous structure of living tissues and assures the proper estimation of temperature.

References

[1] Liu, H.L., Chen, Y.Y., Jen, J.Y., Lin, W.L., Pilot point temperature regulation for thermal lesion during ultrasound thermal therapy, *Medical & Biological Engineering & Computing*, Vol. 42, pp. 178-188, 2004.

[2] Lv, Y.G., Deng, Z.S. and Liu, J., 3D numerical study on the induced heating effects of embedded micro/nanoparticles on human body subject to external medical electromagnetic field, *IEEE Transactions on Nanobioscience*, Vol. 4, No 4, pp. 284-294, 2005.

[3] Majchrzak, E., Numerical solution of dual-phase-lag model of bioheat transfer using the boundary element method, *CMM 2009: Short Papers: 18th International Conference on Computer Methods in Mechanics*, Zielona Góra, pp. 297-298, 18-21 May 2009.

[4] Xu, F., Seffen, K.A. and Lu T.J., Non-Fourier analysis of skin biothermomechanics, *International Journal of Heat and Mass Transfer*, 51, pp. 2237-2259, 2008.

[5] Yuan, P., Numerical analysis of temperature and thermal dose response of biological tissues to thermal non-equilibrium during hyperthermia therapy, *Medical Engineering & Physics*, 20, pp. 135-143, 2008.

[6] Zhou, J., Chen, J.K. and Zhang, Y., Dual-phase lag effects on thermal damage to biological tissues caused by laser irradiation, *Computers in Biology and Medicine*, 39, pp. 286-293, 2009.